Biocybernetics and Biomedical Engineering
2010, Volume 30, Number 3, pp. 19–34

Description of Biomedical Textures by Statistical Properties of Morphological Spectra

JULIUSZ L. KULIKOWSKI*, MAŁGORZATA PRZYTULSKA, DIANA WIERZBICKA

Nałęcz Institute of Biocybernetics and Biomedical Engineering, Polish Academy of Sciences, Warsaw, Poland

A class of mathematical models of biological textures based on the multi-variable probability distributions of their morphological spectra is described. It is shown that a large class of such distributions can be presented by sufficient statistics consisting of the coefficients of their expansion into the series of multi-variable Hermite polynomials. The sufficient statistics can then be simplified by rejection of higher-order terms. The general concepts of mathematical models construction are illustrated by examples of textures of several biological tissues (aorta walls, liver and blood). The role of statistics based on absolute values of morphological spectral components and of their cross-correlation coefficients is underlined.

K e y w o r d s: texture analysis, statistical models, morphological spectra, multivariable Hermite polynomials

1. Introduction

Recognition of textures plays a substantial role in computer-aided analysis of biomedical images aimed at discrimination of tissues or objects characterized by specific micro-morphological structure. Among numerous methods of texture analysis, the spectral, morphological, statistical and fractal methods are the most frequently used and mentioned in literature [1÷7]. However, textures are not strongly defined mathematical objects, so they only can be approximated by less or more adequately chosen formal models. The models should, in particular, reflect such typical properties of biological textures as their irregularity, spatial heterogeneity and multi-scalar

* Correspondence to: Juliusz L. Kulikowski, Nałęcz Institute of Biocyberntics and Biomedical Engineering, Polish Academy of Sciences, ul. Ks. Trojdena 4, 02-109 Warsaw, Poland, e-mail: juliusz.kulikowski@ibib.waw.pl
Received 4 September 2009; accepted 8 March 2010

structure. *Irregularity* means that no large area segments of texture can be exactly represented by a functional extension of smaller area segments and thus the amount of information necessary for an exact description of the texture covering a part of an image is growing up with the area of this part. Not all textures are irregular; however, most of textures available in biomedical or geophysical observations are irregular. *Spatial heterogeneity* means that texture characteristics are not fixed in large image areas but are continuously changing without clearly visible borders. *Structural multi-scalarity* of texture means a dependence of texture characteristics on the resolution of image presentation. For example, the texture of a forest visible in an aero-photo is different than this of a single tree observed from a small distance and this one is different than that of a single leaf surface.

Morphological spectra (*MS*) are one of the concepts useful in construction of formal texture models satisfying the above-mentioned requirements [8, 9]. Application of *MS* is limited to the analysis of monochromatic images given in the form of finite, $I \times J$-size bitmaps, I and J being some natural numbers denoting, respectively, the number of rows and columns of the bitmap. The elements of the bitmap (pixel brightness levels) are limited non–negative real numbers; in computer image processing systems they are declared as integers. *MS* are closely related to the systems of orthogonal $2D$ Walsh functions [10], however, there are also substantial differences between *MS* and Walsh functions based approach to texture analysis, as shown in Table 1. In principle, *MS* can be extended to higher, $3D$ or $2D + 1$ dimensions in order to describe volume- or time-dependent textures; however, the calculation costs grow exponentially with the dimensionality. Below, $2D$ images only and their *MS* are considered.

Table 1. Comparison of 2D Walsh functions and morphological spectra

Property \ Type of representation	Systems of Walsh functions	Morphological spectra
Image format	fixed	extendable
Image resolution	unlimited	fixed
Description of components	functional	algebraic
Components calculation ordering	bottom-up	top-down
Interpretation of basic geometrical objects' transformations	possible	easy
Image filtering possibility	through reverse transformation	through reverse transformation or directly

Despite the *MS* dimensionality, their properties are determined by a natural parameter n called *MS level*. In principle, any level of *MS* of an image contains complete information making exact reconstruction of the original image possible. However, n determines the minimum size of image that by the n-th level *MS* can be represented, because it should not be smaller than a single $2^n \times 2^n$ pixels square, called *basic window,* size. Therefore, it is reasonable to choose n so as to cover, with limited margins, the $I \times J$-size image by a finite number of the basic windows. The

contents of a n-th level basic window is represented by $k = 4^n$ *MS* components. If N denotes the number of basic windows covering a certain image area, then $N \cdot 4^n$ is the number of *MS* components representing it. A hierarchical structure of *MS* components is illustrated in Fig. 1.

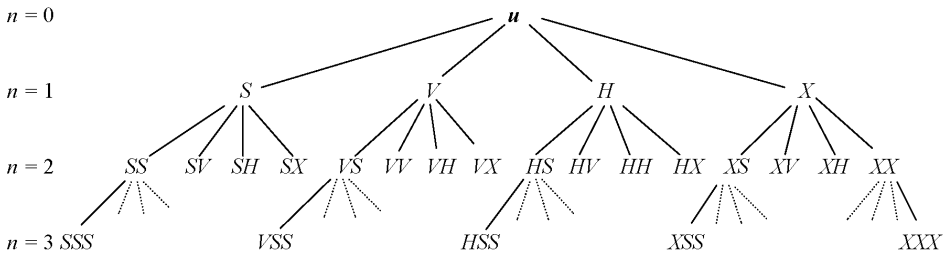

Fig. 1. Hierarchical tree of *MS* components

The symbols *S, V, H* and *X* used here are assigned to four basic operations performed on the basic operations generating the higher-n *MS* components on the basis of the lower-n ones: a sum (*S*) and the differences of the vertical (*V*), horizontal (*H*) and diagonal (*X*) sums of 2×2 square matrix elements [8, 9].

The aim of this paper is to present statistical models of textures based on their morphological spectra. The models are illustrated by the textures of selected biological tissues: of aorta walls (as an example of anisotropic tissue) and of liver section (isotropic tissue). The paper is organized as follows: basic assumptions concerning statistical description of textures based on morphological spectra are presented in Sec. 2. In Sec. 3 the experimental results of analysis of selected textures analysis are given.

2. Statistical Models of Texture Based on Morphological Spectra

A statistical description of textures is based on the following assumption:

A texture covering a fixed image area can be considered as an instance of a 2D random field, whose local statistical properties are homogenous in the given area within an admissible accuracy interval.

The assumption holds thus within the limits forced by large-scale spatial heterogeneity of the texture. Using *MS* as a tool for texture description leads to an additional assumption:

a fixed texture observed in a given image area can be represented by a set of instances of random MS components, statistically independent in basic windows covering the area.

The basic window are assumed to be of a square form and of $2^n \times 2^n$ size, strongly connected with the *MS* level n, as illustrated in Fig. 2. An original view of

a texture given in the form of its *MS* components in a set of basic windows can be easily obtained by a *MS* reverse transformation [9].

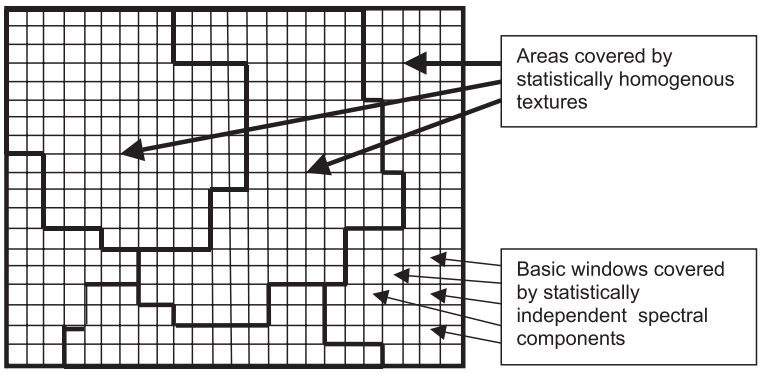

Fig. 2. Image segmentation into basic windows and statistically homogenous areas

According to the above-formulated notions it is assumed as follows:

A statistical model of a texture θ in a narrow sense is given by a conditional probability distribution of a multidimensional random value Ξ describing measurable texture parameters, assuming that θ has been chosen from a family Θ of admissible textures.

In the case of using of *MS* to texture description, Ξ is interpreted as a random vector of spectral components belonging to k-dimensional linear vector space R^k, where $k = 4^n$. High dimensionality of Ξ for large n makes exact description of its probabilistic properties an onerous task. Thus, it is necessary to find suitable approximations of the multidimensional probability distribution function (*pdf*). One of the possibilities consists in *pdf* expansion into multi-variable Hermite polynomials [10].

Let $\xi = [\xi_1, \xi_2, ..., \xi_k]$ be a vector of observed k components of *MS* considered as instances of Ξ. It follows from the former considerations that standard values of k are 4^n for $n = 1,2,3,\ldots$ etc. A class of conditional probability densities (*cpd*) of Ξ for fixed θ will be considered. Assuming that all its finite moments exist we shall denote by:

$\mu(\theta) = [\mu_1, \mu_2, \ldots, \mu_k]$ – a vector of mean values of the *MS* components,
$[\sigma_{ij}(\theta)]$ for $i,j = 1,2,\ldots,k$, $\sigma_{ii} > 0$, – a covariance matrix of the *MS* components.
Then, Ξ can be replaced by a random vector $\boldsymbol{Z}$ of normalized variables:

$$Z_i = \frac{\xi_i - \mu_i}{\sigma_{ii}}, \quad i = 1, 2, ..., k. \tag{1}$$

By $\boldsymbol{z} = [z_1, z_2, ..., z_k]$ a vector of observed values (instances) of $\boldsymbol{Z}$ will be denoted and by $w_k(\boldsymbol{z}|\theta)$ – a *cpd* describing its probabilistic properties. Then the *cpd* can be expanded into a series of Hermite polynomials:

$$w_k(\mathbf{z}\,|\,\theta) = \frac{1}{(2\pi)^{\frac{k}{2}}\sqrt{|\,\rho_{ij}\,|}} e^{[-\frac{1}{2}Q(z)]} \sum_{r=0}^{\infty} \sum_{m+n+...+p=r} \frac{1}{m!n!...p!} b_{m,n,...,p}(\theta) \qquad (2)$$
$$H_{m,n,...,p}(z)$$

where

$$Q(\boldsymbol{z}) = \boldsymbol{z} \cdot [\rho_{ij}(\theta)]^{-1} \cdot \boldsymbol{z}^{tr} \qquad (2a)$$

is a square-form of the normalized *MS* components, $[r_{ij}]$ is a cross-correlation matrix of Ξ:

$$\rho_{ij} = \frac{\sigma_{ij}}{\sqrt{\sigma_{ii}\sigma_{jj}}}, \quad i,j = 1,2,...,k, \qquad (2b)$$

$$H_{m,n,...,p}(\mathbf{z}) = (-2)^{m+n+...+p} \exp[\frac{1}{2}Q(\mathbf{z})] \frac{\partial^{m+n+...+p}}{\partial^m z_1 \partial^n z_2 ... \partial^p z_k} \exp[-\frac{1}{2}Q(\mathbf{z})] \qquad (2c)$$

denotes a $(m,n,...,p)$-th order Hermite polynomial;

$b_{m,n,...,p}(\theta)$ are quasi-moments, i.e. mean values of the conjugate Hermite polynomials $G_{n,m,...,p}(\boldsymbol{z})$:

$$b_{m,n,...,p}(\theta) = \int_{\infty}^{\infty} w_k(\mathbf{z}\,|\,\theta) G_{m,n,...,p}(\mathbf{z}) d\mathbf{z}, \qquad (2d)$$

$$G_{m,n,...,p}(\mathbf{z}) = (-\frac{1}{2})^{m+n+...+p} \exp[\frac{1}{2}Q^*(\mathbf{z})] \frac{\partial^{m+n+...+p}}{\partial^m z_1 \partial^n z_2 ... \partial^p z_k} \exp[-\frac{1}{2}Q^*(\mathbf{z})], \qquad (2e)$$

$$Q^*(\boldsymbol{z}) = \boldsymbol{z} \cdot [\rho_{ij}(\theta)] \cdot \boldsymbol{z}^{tr}. \qquad (2f)$$

It should be noticed that all the *cpd* parameters: $b_{m,n,...,p}(\theta)$, $\mu(\theta)$, $\sigma_{ij}(\theta)$, $\rho_{ij}(\theta)$ depend on θ as on texture's features. From (2c) it follows that: 1^0 for $k = 1$ the first Hermite polynomials have the form: $H_0(z) = 1$, $H_1(z) = 2z$, $H_2(z) = 4z^2 - 2$, $H_3(z) = 8z^3 - 12z$, etc., 2^0 for $k > 0$ and $r = 0$ it is: $H_{0,0,...,0}(\boldsymbol{z}) \equiv 1$, 3^0 for $k > 0$ and $r = 1$ it is $H_{0,0,...,1,...,0}(z) = 2\Sigma^k_{i=1}\rho_{pi}z_i$ (p is the position whose index is 1), etc. Hence, a first approximation of $w_k(\boldsymbol{z}|\theta)$ is given by a k-variable Gaussian distribution of the *MS* components. Moreover, it follows from (2) and (1c) that the correcting terms in formula (2) corresponding to $r = 1$ and $r = 2$ equal 0 due to the normalization of z. The first non-zero correcting terms caused by the asymmetry of *pdf* correspond to $r = 3$; they are represented by algebraic combinations of the moments of z_i^3, $z_i^2 z_j$ and $z_i z_j z_l$-type for $i,j,l = 1,2,\ldots,k$. Next terms, corresponding to $r = 4, 5,\ldots$ etc., contribute to the *pdf* form; however, their role is the lower the higher the similarity between the approximated *pdf* and the Gaussian function is.

Let us denote by $\mathbf{S} = [\sqrt{\sigma_{ii}\sigma_{jj}}\rho_{ij}]$ a covariance matrix, by $\mathbf{M}^{(3)} = [\sqrt{\sigma_{ii}\sigma_{jj}\sigma_{ll}} \cdot \rho_{ijk}]$ – a matrix of 3rd order moments, by $\mathbf{M}^{(4)} = [\sqrt{\sigma_{ii}\sigma_{jj}\sigma_{ll}} \cdot \rho_{ijk}]$ – a matrix of 4th order moments of the variables $z_1, z_2, \ldots, z_k$, etc. (for the sake of simplicity, the dependence of the parameters on θ being here omitted). From the fact that any r-th order Hermite polynomial is an algebraic combination of the up to r-th order moments, it follows that for a given r full information about the *pdf* form is contained in the sets of parameters shown in Table 2. Thus, the parameters can be displayed in the form of linear vectors which will be denoted by $\boldsymbol{\Phi}^{(r)}(\theta)$, r = 1, 3, 4, 5,… Therefore, the following holds:

Statistical models of a texture θ in a wide sense are given by approximations of sufficient statistics of conditional probability distribution of the random value Ξ describing measurable texture parameters, assuming that θ has been chosen from a family Θ of admissible textures.

Table 2. Sufficient statistics' approximations given by the sets of parameters

r	**Parameters of *pdf***
1	$\boldsymbol{\mu}(\theta), \boldsymbol{S}(\theta)$
3	$\boldsymbol{\mu}(\theta), \boldsymbol{S}(\theta), \mathbf{M}^{(3)} = [\sqrt{\sigma_{ii}\sigma_{jj}\sigma_{ll}} \bullet \rho_{ijl}]$
4	$\boldsymbol{\mu}(\theta), \boldsymbol{S}(\theta), \mathbf{M}^{(3)} = [\sqrt{\sigma_{ii}\sigma_{jj}\sigma_{ll}} \bullet \rho_{ijl}], \mathbf{M}^{(4)} = [\sqrt{\sigma_{ii}\sigma_{jj}\sigma_{ll}\sigma_{mm}} \bullet \rho_{ijlm}]$
5	$\boldsymbol{\mu}(\theta), \boldsymbol{S}(\theta), \mathbf{M}^{(3)} = [\sqrt{\sigma_{ii}\sigma_{jj}\sigma_{ll}} \bullet \rho_{ijl}], \mathbf{M}^{(4)} = [\sqrt{\sigma_{ii}\sigma_{jj}\sigma_{ll}\sigma_{mm}} \bullet \rho_{ijlm}], \mathbf{M}^{(4)} = [\sqrt{\sigma_{ii}\sigma_{jj}\sigma_{ll}\sigma_{mm}} \cdot \rho_{ijlm}]$

etc.

Example 1

Consider a 1st order (n = 1) *MS* of a texture whose *pdf* has been approximated by the first (r = 1) term of the formula (2). The *MS* then contains $k = 4^n = 4$ components which can be denoted by z_S, z_V, z_H, z_X. If a first term approximation of $w_k(z_S, z_V, z_H, z_X|\theta)$ is chosen then it is fully characterized by $\boldsymbol{\mu}(\theta)$ and $\boldsymbol{S}(\theta)$ only. Thus, $\boldsymbol{\mu}(\theta) = [\mu_S(\theta), \mu_V(\theta), \mu_H(\theta), \mu_X(\theta)]$ consists of 4 parameters while $\boldsymbol{S}(\theta) = [\sigma_{ij}(\theta)]$, $i,j \in \{S, V, H, X\}$, due to its symmetry, consists of $½ \cdot 4 \cdot 5 = 10$ parameters. Thus, the corresponding vector of parameters will have the following form (the dependence on θ being omitted below):

$$\boldsymbol{\Phi}^{(1)} = [\mu_S, \mu_V, \mu_H, \mu_X, \sigma_{SS}, \sigma_{SV}, \sigma_{SH}, \sigma_{SX}, \sigma_{VV}, \sigma_{VH}, \sigma_{VX}, \sigma_{HH}, \sigma_{HX}, \sigma_{XX}].$$

If the above-mentioned parameters are replaced by their estimates calculated from observations then $\boldsymbol{\Phi}^{(1)}$ can be interpreted as sufficient statistics for estimation of $w_k(z_S, z_V, z_H, z_X|\theta)$ ●

The number of components of the sufficient statistics $\boldsymbol{\Phi}^{(r)}$ increases exponentially with n and r as shown in Table 3 ($n = 0$ corresponds to a *pdf* of any selected single spectral component). It might seem from the Table that in general, despite the fact that higher-level *MS* make it possible to inspect the existence directly and form of larger morphological structures, using sufficient statistics corresponding to higher n or r for texture analysis is unreasonable. However, it is not quite so if the below-described multi-scalar properties of *MS* are taken into account.

Table 3. Number of parameters of sufficient statistics

n \ r	1	3	4
0	2	3	4
1	14	34	69
2	152	968	4844
3	2144	47844	814324

The 2nd level components *SS, VS, HS* and *XS* divided by 4 can also be interpreted as 1st level components of the same image whose resolution power has been reduced by 2 (each pixel value being equal to 4 original pixel values forming a square). Similarly, the 3rd level components *SSS*, *SSV, SSH* and *SSX* divided by 16 are equivalent to 1st level components of the image whose resolution power has been reduced by 4, etc. Therefore, the 2nd level *MS* makes us able also to analyze some properties of the 1st level *MS*. This possibility has been used to compare the *pdf*-s of 1st level *MS* of selected tissues whose statistics has been limited by fixing the parameters $r = 1$ and $n = 0$ and 1 (see Table 3).

3. Statistical Experiments

In order to prove the validity of using of *MS* to texture analysis in medical diagnosis several experiments have been done [9, 12, 13]. The investigations were limited to arbitrarily chosen lower-level spectral components and have shown that the method needs deeper examination of statistical properties of complete *MS* for some typical textures. Below, main results of such examinations are presented.

The textures of three types of human biological tissues were used: a) aorta as an example of fibrous tissue, b) liver and c) fetal blood as examples of granular tissues. In addition, the anisotropic texture of aorta tissue were observed in three positions: *a*') vertical, *a*") rotated by 30^0 and *a*"') horizontal. The patterns visible in *a*') and *a*"') are similar while this in *a*") is different as being obtained by an independent digitization of a rotated image. Totally, this gave us 5 types of tissue images shown in Fig. 3 for calculation of *MS* and their statistical examination.

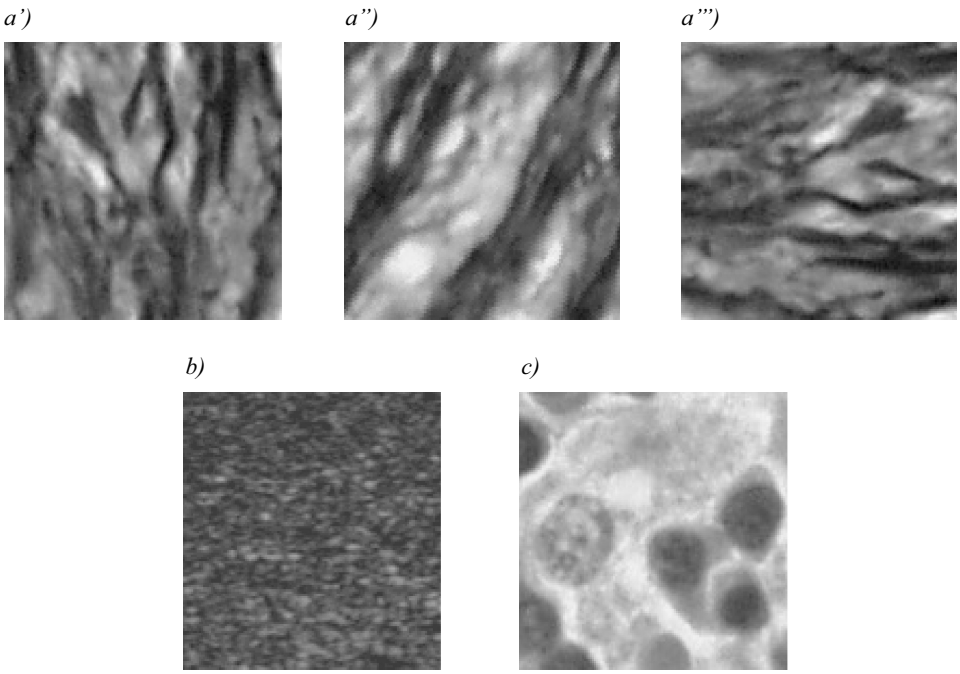

Fig. 3. Textures used in statistical experiments: *a'), a"), a"')* – aorta in different angular orientations, *b)* liver tissue, *c)* fetal blood tissue

The images are of 128 × 128 pixels size. They were examined by using 2nd level ($n = 2$) *MS* i.e. by partition into 4 × 4 pixels size basic windows. *MS* consists in this case of 16 components; moreover, as follows from Fig. 1, all higher- and/or lower-level *MS* components can be calculated on their basis. Statistical error of *MS* components' estimation depends on the number of basic windows covering the given image sector. In the below-analyzed case the numbers are: 4096 for $n = 1$, 1024 for $n = 2$, 256 for $n = 3$, 64 for $n = 4$, etc.

Experiment 1

For $r = 0$ (*pdf* of a single *MS* component) there were considered the *SS* components (representing the luminance level of pixels) of liver and blood tissue. The images are of different average luminance and of different granularity (see Fig. 3*b* and 3*c*). There were calculated the histograms of the given *MS* component as shown in Fig. 4.

Not only different positions of the histograms caused by the difference of mean luminance levels can be observed, but also a difference of forms; the more extended and bimodal form of the blood texture is caused by existence in the image of dark large morphological structures on bright background. The difference is also reflected by the entropies of the histograms: 467.17 bits for liver and 1166.9 bits for blood tissues.

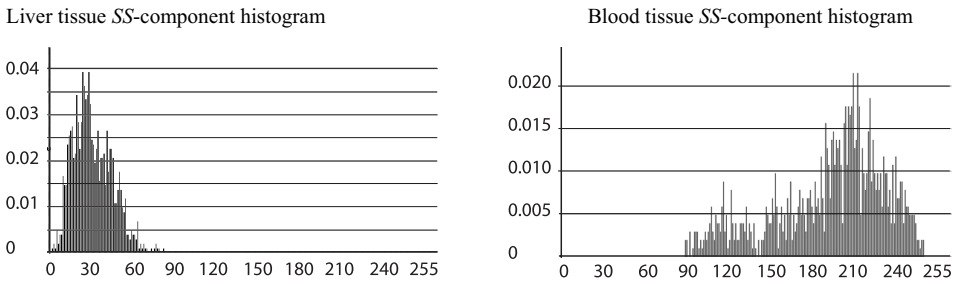

Fig. 4. Comparison of liver and fetal blood tissue *SS*-component histograms (presented in comparable scales)

Experiment 2

A dependence of the sign of *MS* components (except the *SS* ones) on vertical and/or horizontal image shifts within the basic windows [8], which is important in exact image reconstruction in texture analysis is a rather undesirable *MS* property. In order to make the texture recognition insensitive to small parallel image shifts, the absolute values of *MS* components instead of the real ones should be taken into account. In this experiment the mean values and variances of 2nd level *MS* components of liver tissue texture were calculated. In Fig. 5 the estimated real and absolute mean values of *MS* components in increasing order are presented. It should be remarked that 1st the absolute values are higher than the real ones, and 2nd the order of components in both cases are different:

real: *XV, VH, XX, HH, VV, XS, HV, XH, HS, VS, SS, SX, VX, SH, SV, HX*
absolute: *XV, XS, XH, XX, VH, HV, VS, VV, SS, HS,VX, HH, HX, SX, SV, SH.*

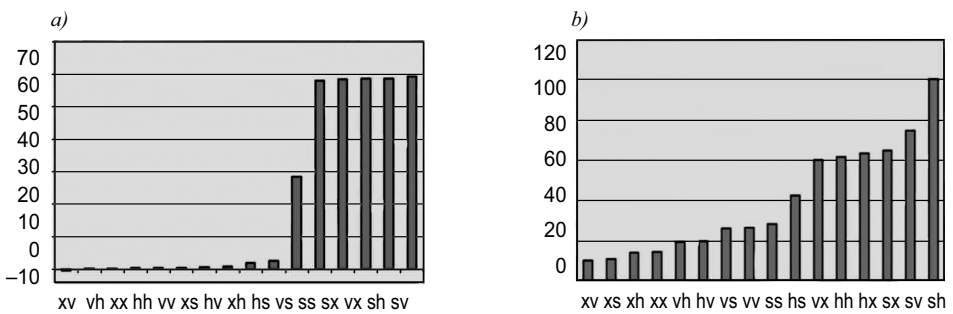

Fig. 5. Mean values of *MS* components of liver tissue texture (in comparable scales): *a*) real, *b*) absolute

A similar comparison of variances of the *MS* components' real and absolute values gave the results shown in Fig. 6. In this case the variances of the absolute *MS* components' values are in general lower than those of the real ones. The orders are also different:

real: *SS, XV, XS, XH, XX, HV, VH, VV, VS, VX, HX, HS, SX, SV, HH, SH*
absolute: *XV, XS, XH, XX, SS, HV, VH, VV, VS, HS, VX, HX, SX, HH, SV, SH.*

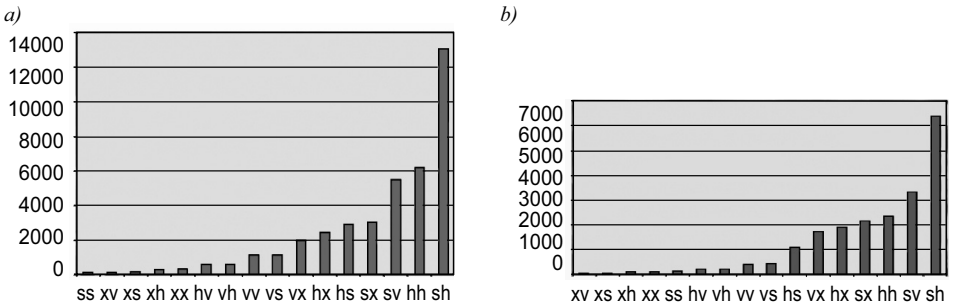

Fig. 6. Variances of *MS* components of liver tissue texture. Vertical scales in *a*) real and *b*) absolute diagrams have been presented so as to make the heights of the pairs of the corresponding components comparable

Despite the fact that neglecting the signs of *MS* components reduces the amount of information, absolute *MS* components provide a more valuable information which is independent of the parallel shifts of the image.

Experiment 3

There were estimated the parameters characterizing the *pdf*-s of absolute 1st level *MS* components' values of the five textures shown in Fig. 1 after reduction of their resolution power by 2. The statistics have been then established by the parameters $n = 1$, $r = 1$. Therefore, according to Table 2 the following 14 parameters were estimated:

a) mean values: $\mu_{|S|}$, $\mu_{|V|}$, $\mu_{|H|}$, $\mu_{|X|}$,

b) covariances: $\sigma_{|SS|}$, $\sigma_{|SV|}$, $\sigma_{|SH|}$, $\sigma_{|SX|}$, $\sigma_{|V,V|}$, $\sigma_{|VH|}$, $\sigma_{|VX|}$, $\sigma_{|HH|}$, $\sigma_{|HX|}$, $\sigma_{|XX|}$.

The results are shown in Table 4. It can be observed that:

1. The cross-correlations between the spectral components $|S|$, $|V|$, $|H|$ and $|X|$ are much below their variances which means that in the considered textures the statistical dependencies between spectral components can be neglected at the first approximation level;

Table 4. Statistical parameters of absolute *MS* components of selected textures

$\boldsymbol{\Phi}^{(1)}$ / θ	$\mu_{\|S\|}$	$\mu_{\|V\|}$	$\mu_{\|H\|}$	$\mu_{\|X\|}$	$\sigma_{\|SS\|}$	$\sigma_{\|SV\|}$	$\sigma_{\|SH\|}$	$\sigma_{\|SX\|}$	$\sigma_{\|VV\|}$	$\sigma_{\|VH\|}$	$\sigma_{\|VX\|}$	$\sigma_{\|HH\|}$	$\sigma_{\|HX\|}$	$\sigma_{\|XX\|}$
a'	27.32	15.14	7.18	1.60	78.66	0	0.01	0	172.9	0.012	0.01	35.93	0.01	1.84
a''	31.96	13.51	9.94	3.99	139.0	0	0.01	0.01	129.0	0.025	0.02	73.11	0.02	10.72
a'''	27.32	7.18	15.14	1.60	78.66	0	0.01	0	35.9	0.012	0.01	172.9	0.01	1.84
b	7.11	6.59	10.61	2.74	10.22	0	0	0	28.2	–0.003	0	69.5	0	4.20
c	43.81	8.69	7.79	1.29	84.4	0	0	0.01	66.0	0.017	0	52.25	0.01	1.29

2. There is a symmetry between the textures denoted by *a*' and *a*''' (obtained by rotation by 90^0) with respect to a permutation of the indexes *V* and *H* (following from the general *MS* properties);

3. The vector $\boldsymbol{\Phi}^{(1)}(a''')$ due to the components $\mu_{|V|}$, $\mu_{|H|}$, $\sigma_{|VV|}$ and $\sigma_{|HH|}$ is closer to $\boldsymbol{\Phi}^{(1)}(a')$ than to $\boldsymbol{\Phi}^{(1)}(a'')$. This corresponds to the fact that for *a', a''* and *a'''* representing the same tissue in different spatial orientations the dilation angle between *a'* and *a''* is smaller (30º) than this between *a''* and *a'''* (60^0);

4. For the vectors $\boldsymbol{\Phi}^{(1)}$ the relative variations coefficient:

$$\gamma = (\mu_{|V|} + \mu_{|H|} + \mu_{|X|})/\mu_{|S|}, \tag{3}$$

was calculated. This gave the results shown in Table 5:

Table 5. Relative variations coefficients of selected textures

θ	*a'*	*a''*	*a'''*	*b*	*c*
γ	0.875	0.858	0.875	2.804	0.405

It can be remarked that the highest value of γ corresponds to the texture *b* characterized by existence of the smallest morphological structures (see Fig. 3). This suggests that in the case of adequately chosen *MS* level the relative variations coefficient can be used as a statistical measure of texture's granularity.

Experiment 4

It was shown (see Table 3) that sufficient statistics for examination of 2nd level *MS* basically consists of at least 152 parameters including 16 1st order and 136 2nd order moments. Examination of a full cross-correlation matrix $\boldsymbol{R}(\theta)$ can also be a basis of *MS* components' informational value evaluation. The matrices $\boldsymbol{R}(\theta)$ were calculated for $\theta \in \{a', a'', a''', b, c\}$. Examples of several series of cross-correlation coefficients ρ_{pq} between the *MS* components of the *a''* tissue are shown in Fig.7. In fact, the full 2nd order *MS* consists of 16 components and the cross-correlation matrix of the components is of 16 x 16 size, its main-diagonal elements being equal 1. The cross-correlation values are presented in increasing order for better visualization of the range of differences between the cross-correlations. The lengths of the rows is decreasing because the symmetry of the cross-correlation coefficients was taken into account; the diagonal elements ρ_{pp} (equal 1 by definition), have been neglected in the graphs.

The increasing order of the cross-correlations between the *MS* components contain an important information about their validity for tissue recognition. For this purpose the groups of strongly mutually correlated *MS* components with a negligible loss of recognition accuracy can be replaced by their algebraic combinations. In Table 6 all pairs of the *MS* components ordered according to the increasing order of their cross-correlation coefficients are presented. First four rows of this Table indicate the order of components held also in the horizontal elements shown in Fig. 7 a,b,c,d. Generally

speaking, the larger the row-distance of a *MS*-component to the corresponding diagonal element is the higher the cross-correlation between the components is.

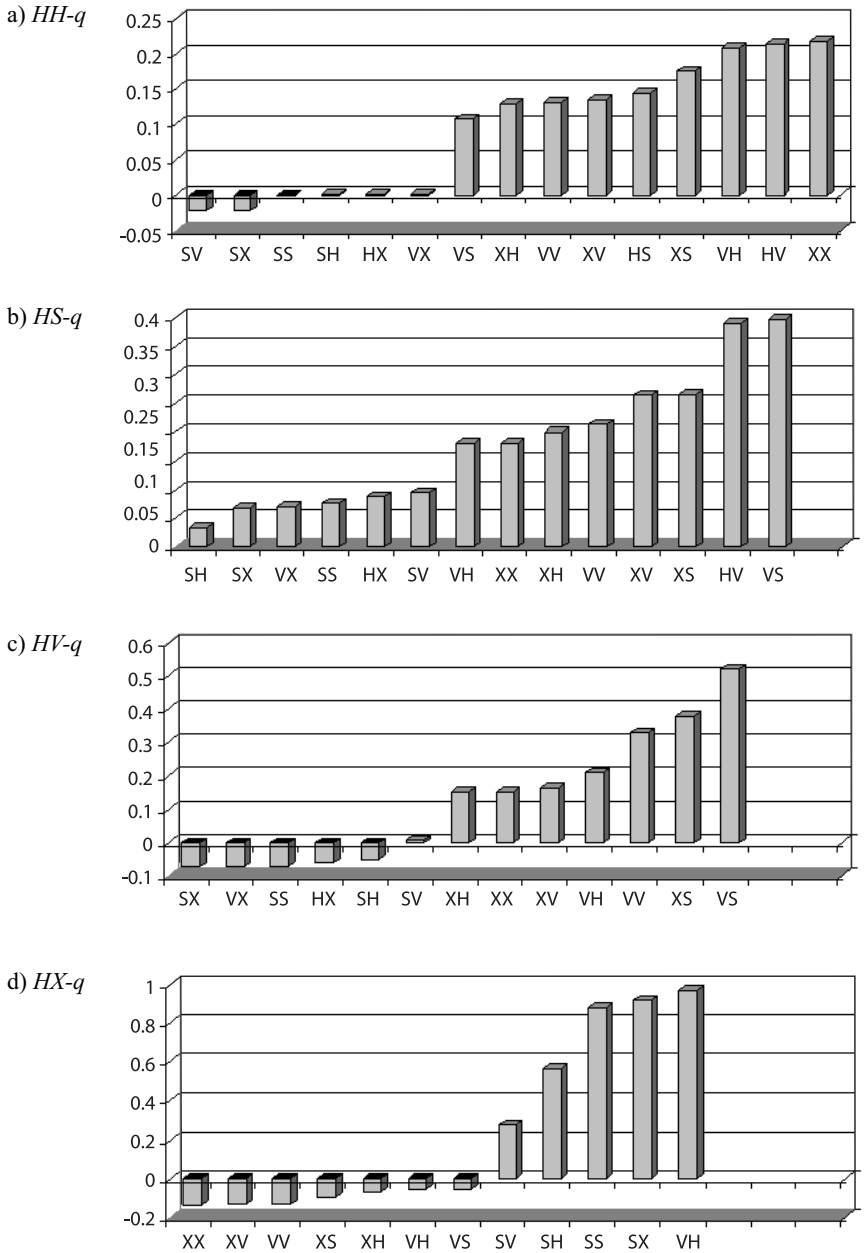

Fig. 7. Cross-correlation values between the 2nd level *MS* components in *a"* (aorta tissue) image. (for denotations of horizontal coordinates see Table 6)

Table 6. Order of increasing cross-correlations between the 2nd level *MS* components

	# *p-q* *p-*	15	14	13	12	11	10	9	8	7	6	5	4	3	2	1
a)	*HH-*	*SV*	*SX*	*SS*	*SH*	*HX*	*VX*	*VS*	*XH*	*VV*	*XV*	*HS*	*XS*	*VH*	*HV*	*XX*
b)	*HS-*	–	*SH*	*SX*	*VX*	*SS*	*HX*	*SV*	*VH*	*XX*	*XH*	*VV*	*XV*	*XS*	*HV*	*VS*
c)	*HV-*	–	–	*SX*	*VX*	*SS*	*HX*	*SH*	*SV*	*XH*	*XX*	*XV*	*VH*	*VV*	*XS*	*VS*
d)	*HX-*	–	–	–	*XX*	*XV*	*VV*	*XS*	*XH*	*VH*	*VS*	*SV*	*SH*	*SS*	*SX*	*VX*
e)	*SH-*	–	–	–	–	*XS*	*VV*	*XV*	*XX*	*VH*	*HX*	*VS*	*VX*	*SX*	*SV*	*SS*
f)	*SS-*	–	–	–	–	–	*XS*	*VV*	*XX*	*XV*	*VH*	*SV*	*VS*	*XH*	*VX*	*SX*
g)	*SV-*	–	–	–	–	–	–	*XS*	*XH*	*XX*	*XV*	*VV*	*VH*	*VS*	*VX*	*SX*
h)	*SX-*	–	–	–	–	–	–	–	*VV*	*XX*	*XV*	*XS*	*XH*	*VH*	*VS*	*VX*
i)	*VH-*	–	–	–	–	–	–	–	–	*VX*	*XH*	*VS*	*XV*	*XX*	*XS*	*VV*
j)	*VS-*	–	–	–	–	–	–	–	–	–	*VX*	*XX*	*XH*	*XV*	*XS*	*VV*
k)	*VV-*	–	–	–	–	–	–	–	–	–	–	*VX*	*XS*	*XV*	*XH*	*XX*
l)	*VX-*	–	–	–	–	–	–	–	–	–	–	–	*XH*	*XS*	*XV*	*XX*
m)	*XH-*	–	–	–	–	–	–	–	–	–	–	–	–	*XV*	*XS*	*XX*
n)	*XS-*	–	–	–	–	–	–	–	–	–	–	–	–	–	*XX*	*XV*
o)	*XV-*	–	–	–	–	–	–	–	–	–	–	–	–	–	–	*XX*

Having given a sample of a texture, deciding, which of its *MS* components are the most suitable to the texture characterization is not a simple task. The widely known method of reduction of the sets of physical objects describing parameters, used in pattern recognition, is based on the calculation and analysis of the Eigen-values and Eigen-vectors of the covariance matrix $\boldsymbol{S}(\theta)$ [14]. However, the example shows that a rough solution of this problem can be based on a primary analysis of the increasing order of cross-correlation coefficients of the parameters (which, so or so, for exact solution also should be calculated). Of course, in each case of texture analysis a subset of the most suitable for a given texture characterization *MS* components may be different. In the above-presented case the highest cross-correlations were observed between the pairs (*p-q*) of *MS* components shown in Table 7.

Table 7. The highest cross-correlations between the pairs of *MS* components

p-q	*VX-HX*	*SX-HX*	*SX-VX*	*SS-SX*	*SS-HX*	*SS-VX*	*SS-SH*	*SV-SH*	*SH-SX*	*SH-HX*	*SH-VX*
σ_{pq}	0.97	0.92	0.92	0.91	0.88	0.87	0.79	0.60	0.58	0.57	0.54

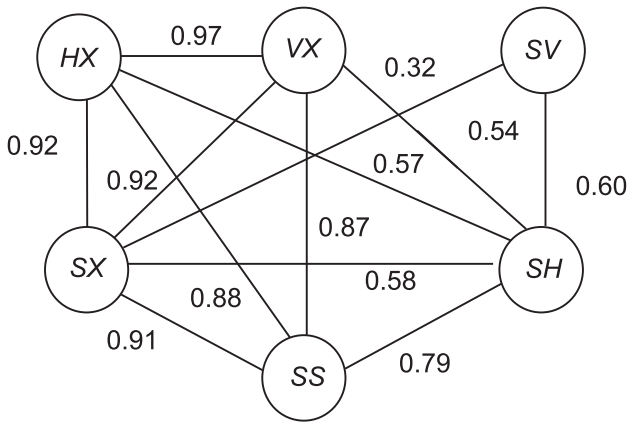

Fig. 8. A graph of the highest cross-correlations between the pairs of *MS* components

These relationships can also be illustrated by a graph of cross-correlations shown in Fig. 8.

Analysis of the graph shows that the modules $|SS|$, $|SX|$, $|VX|$ and $|HX|$ of *MS* components are mutually strongly correlated. This suggests that for characterizing of the given type of texture (*a"*) a reduced statistic:

$$Z = |SS| + |SX| + |VX| + |HX| \tag{4}$$

instead of its separate components without a substantial loss of information can be used. However, a reduction of sufficient statistics for several textures discrimination purpose is possible only if the same clusters of *MS* components in all discriminated textures occur. In particular, in texture analysis based on higher-level *MS* such clusters should correspond to subsets of morphological micro-structures invariant with respect to parallel translations.

4. Conclusions

Morphological spectra are a general, theoretically well-founded tool for texture analysis. However, like other general tools (e.g. Fourier spectra, Markov fields, fractals, etc.) they should be modified in order to become more effective in the given individual texture analysis problems. Most of textures analyzed in biomedical applications can be considered as random fields. The corresponding mathematical models may have the form of conditional probability distributions or of such distributions representing sufficient statistics. The probability distributions may concern various types of parameters describing the texture, one of them being the *MS* components.

Even having this point established there remain the problems: what *MS* level, which *MS* components or their algebraic combinations, on what statistical accuracy level should be established in order to make the texture analysis effective. In this paper it has been shown and illustrated by examples that using the modules or using the sums of selected modules of *MS* components instead of *MS* real values may lead to better results in statistical characterization of the classes of the textures satisfying some geometrical transformation invariance conditions. Analysis of cross-correlations between the modules of *MS* components gives also an inspection into statistical dependencies between them and may suggest possible ways of reduction of the number of parameters necessary to describe the given class of textures. However, the problem of informative value of higher-level moments describing the non-Gaussian probability distributions of random *MS* components is still not quite clear and needs deeper investigations.

Acknowledgments

This work was performed within the Project 2.4/St/2009 sponsored by the Ministry of Science and Higher Education of Poland. The Authors would like to thank the Reviewer of this paper for the substantial suggestions and critical remarks.

References

1. Zaremba M.B., Palenichka R.M., Missaoui R.: Multi-Scale Morphological Modeling of a Class of Structural Texture. Machine Graphics and Vision 2005, 14, 2, 2005, 171–199.
2. Arasteh S., Hung C-C.: Color and Texture Image Segmentation Using UniformLocal Binary Patterns. Machine Graphics and Vision 2006, 15, 3/4, 265–274.
3. Manjunath B., Chellappa R.: Unsupervised Texture Segmentation Using Markov Random Fields. IEEE Trans. Pattern Analysis and Machine Intelligence 1991, 13, 5, 478–482.
4. Laine A., Fan J.: Texture Classification by Wavelet Packet Signatures. IEEE Trans. Pattern Analysis and Machine Intelligence 1993, 15, 11, 1186–1191.
5. Valkealathi K., Oja E.: Reduced Multidimensional Co-Occurrence Histograms in Texture Classification. IEEE Trans. Pattern Analysis and Machine Intelligence 1998, 20, 1, 90–94.
6. Strzelecki M., Materka A.: Markov Random Fields as Models of Textured Biomedical Images. Proc. of 20th National Conf. Circuit Theory and Electronic Networks KTOiUE'97, Kołobrzeg 1997, 493–498.
7. Smith T.G., Lange G.D.: Biological Cellular Morphometry – Fractal Dimensions, Lacunarity and Multifractals. In: G.A. Losa, D. Merlini et al. (Eds.). Fractals in Biology and Medicine, vol. II, Birkhauser, Basel 1998, 30–49.
8. Kulikowski J.L., Przytulska M., Wierzbicka D.: Recognition of Textures Based on Analysis of Multilevel Morphological Spectra. GESTS Int. Transactions on Computer Science and Engineering, 2007, 38, 1,99–107.
9. Kulikowski J.L., Przytulska M., Wierzbicka D.: Morphological Spectra as Tools for Texture Analysis. In: M. Kurzyński, E. Puchała et al. (Eds.) Computer Recognition Systems 2, Springer-Verlag, Heidelberg, 2007, 510–517.

10. Zalmanzon L.A.: Fourier, Walsh and Haar Transformations, their Applications in Control, Communication and other Domains (in Russian). Nauka, Moscow 1989.
11. Tichonov V.I., Tolkachev A.A.: Abnormal Fluctuations Affecting on Linear Systems (in Russian). Doklady AN SSSR, OTN, No 12, 1956.
12. Kulikowski J.L., Przytulska M.: Biomedical Image Segmentation Based on Morphological Spectra. 4th European Congress of International Federation for Medical and Biomedical Engineering. Antwerpen, Belgium 2008.
13. Przytulska M., Kulikowski J.L., Bajera A., Królicki L.: Comparison of SPECT Cerebral Image Examination Methods Based on Luminance Level and Morphological Spectra Evaluation. Biocybernetics and Biomedical Engineering 2009, 29, 1, 29–42.
14. Pratt W.K.: Digital Image Processing. John Wiley & Sons, New York 2008.